THE BELL SYSTEM TECHNICAL JOURNAL
Vol. 51, No. 8, October, 1972
Printed in U.S.A.

Analysis of a Dual Mode Digital Synchronization System Employing Digital Rate-Locked Loops

By R. W. CHANG

(Manuscript received April 4, 1972)

We examine a data-rate synchronization system capable of operating in two modes: (i) in master-to-slave mode when the data stations are connected by digital transmission facilities, and (ii) in slave-to-slave mode when the data stations are connected by analog transmission facilities. The first part of this paper determines the steady-state behavior and the transient response in the master-to-slave mode. The results show that the system is well behaved in the transient stage, and that the steady-state behavior is satisfactory. From the transient analysis, the buffer size requirements of the system and the counter size requirements of the rate-locked loops are determined. Formulas are developed from which the start-up time of the system can be estimated.

The second part of this paper examines the behavior of the system in the slave-to-slave mode. It is shown that the data stations can settle to the same steady-state signaling rate, and this signaling rate is determined. The dependence of this signaling rate on other system parameters is examined. It is shown that the system can be easily designed such that the steady-state signaling rate will lie within desired limits. (This is so regardless of the starting sequence, the initial system conditions, and time delays in the communication channels.)

I. INTRODUCTION

When data stations are connected by wholly digital transmission facilities, it is most efficient to slave the clocks at the data stations to a master clock. To perform this operation, hereafter referred to as master-to-slave operation, an interface unit at the data station extracts timing pulses from the incoming data stream. These timing pulses are passed through a phase-locked loop to eliminate noise and jitter. The output of the phase-locked loop controls the signaling rate of the data station.

Unfortunately, a technical problem arises when data stations are synchronized in the above manner. Before digital systems evolve into a well-connected network, data stations are also often connected by wholly analog transmission facilities. When two data stations equipped to operate in the master-to-slave mode are connected by analog facilities, each station will regard the clock at the other station as the master clock, and the two stations will attempt to mutually synchronize each other. This mode of synchronization can be called "slave-to-slave." Conventional phase-locked loops[1] which perform well in the master-to-slave mode may not perform well in the slave-to-slave situation, being unusually sensitive to path-length delays and other system parameters. This technical problem can be solved by avoiding the slave-to-slave situation in the following manner:

(*i*) Informing the data stations when analog transmission facilities are used. This will permit the stations to break up the slaving paths in the data sets and use their own clocks as the timing source.

(*ii*) Providing a looped connection within the analog system containing appropriate buffers, and a clock of sufficient accuracy to serve as the master for the data stations.

Unfortunately, these schemes reduce the economic attractiveness of the system. Consequently, there is a need for a synchronization scheme capable of operating in both the master-to-slave and the slave-to-slave modes.

We analyze a synchronization system which employs digital rate-locked loops to determine if it can operate successfully in both modes. The phase detector in the rate-locked loop is a multistage counter that counts the difference between the number of zero crossings of the input signals. Because of this nonlinear counting process, the operation of the synchronization system is determined by nonlinear differential-integral equations. Such equations do not appear in earlier synchronization studies[2-4] which considered different phase detectors. As will be shown, a digital rate-locked loop locks to neither the phase nor the frequency of the timing signal, but to the zero-crossing intervals. This difference complicates the analysis. We have examined the problem without making linear approximations.[5-8] In a previous paper,[9] we analyzed, in a rigorous fashion, the steady-state behavior of the system in the master-to-slave mode and proved that, in the absence of filtering in the rate-locked loop, the slave oscillator will lock to the master oscillator exactly. In this paper, it is proved rigorously that if the

filter in the loop satisfies a simple condition, the system will reach equilibrium (that is, data stations cannot add or delete bits from a customer's data stream). Based on this, it is demonstrated that in the presence of RC filtering in the loop, the slave oscillator will lock to the master oscillator exactly. Following these analyses, this paper determines the transient response of the system in the master-to-slave mode, and examines the behavior of the system in the slave-to-slave mode. Sections II and III of this paper examine the master-to-slave mode. Transient response, buffer-size requirements of the system, and counter-size requirements of the rate-locked loop are determined. Section IV considers the slave-to-slave mode. Steady-state signaling rate of the system is determined, with its dependence on the other system parameters examined. A simple method of designing the system to ensure satisfactory steady-state signaling rate is presented. Section V summarizes the results of this paper and may be read next.

II. MATHEMATICAL MODEL

In this and the following two sections, we examine the master-to-slave mode. Consider two communication stations as depicted in Fig. 1. Station 1 (with slave clock) represents a data station. Station 2 (with master clock) represents a station in the digital transmission facility. The master clock at Station 2 emits a timing signal which controls the transmission of data from Station 2 to Station 1 (for example, Station 2 transmits a digit to Station 1 at every second zero crossing of this timing signal). Station 2 transmits to Station 1 at some standard rate, say, f_2 digits per second.

Station 1 receives data from Station 2, and derives from the received data a timing signal $s_2(t) = \sin(\omega_2 t + \theta_2)$, where $\omega_2 = 2\pi f_2$ and θ_2 is

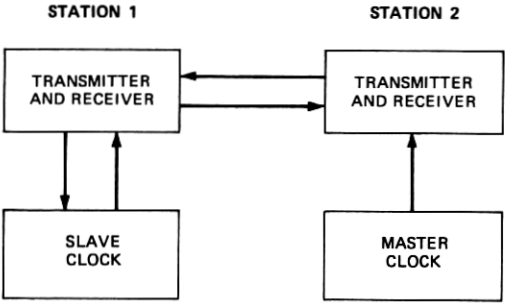

Fig. 1—Master-to-slave operation, block diagram.

an arbitrary phase angle. The signal $s_2(t)$ and the output $s_1(t)$ of a local oscillator are compared in a digital phase detector (Fig. 2). The digital-phase detector is a counter which counts the zero crossings of $s_2(t)$ and $s_1(t)$, and produces an output proportional to the difference between these two counts. Mathematically, this operation can be specified as follows. Let it be assumed that the digital phase detector is activated at $t = 0$. Let $N_1(t)$ and $N_2(t)$ be, respectively, the number of zero crossings (both upward and downward zero crossings) of $s_1(t)$ and $s_2(t)$ in the time interval 0 to t; then the output of the digital phase detector is

$$u_1(t) = e_1[N_2(t) - N_1(t)] \tag{1}$$

where e_1 is a positive constant (volts/count) and may be called the gain of the counter. As depicted in Fig. 2, $u_1(t)$ is passed through a filter, and the filter output $v_1(t)$ controls the frequency of a voltage-controlled oscillator (VCO_1). Let $\omega_1 = 2\pi f_1$ be the free-running radian frequency of VCO_1, then the output of VCO_1 is

$$s_1(t) = \sin\left[\omega_1 t + \alpha_1 \int_0^t v_1(\tau)\, d\tau + \theta_1\right] \tag{2}$$

where α_1 is the gain of VCO_1 (radians/volt $\times$ second). The signal $s_1(t)$ is used to control the transmission of data from Station 1 to Station 2 (for example, Station 1 transmits a digit to Station 2 at every 2nd zero crossing of $s_1(t)$). Note that θ_1 in (2) represents the phase of $s_1(t)$

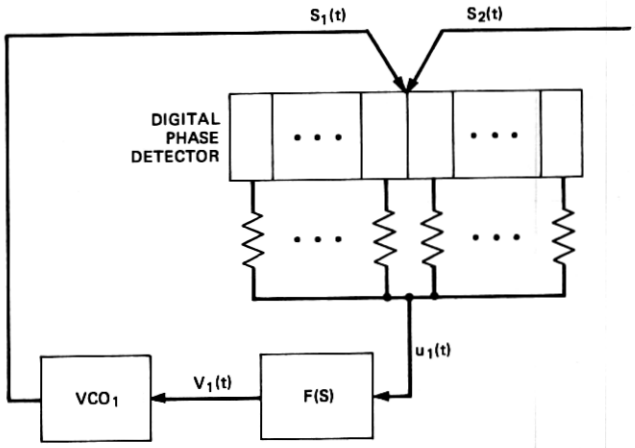

Fig. 2—Digital phase detector and the rate-locked loop at Station 1.

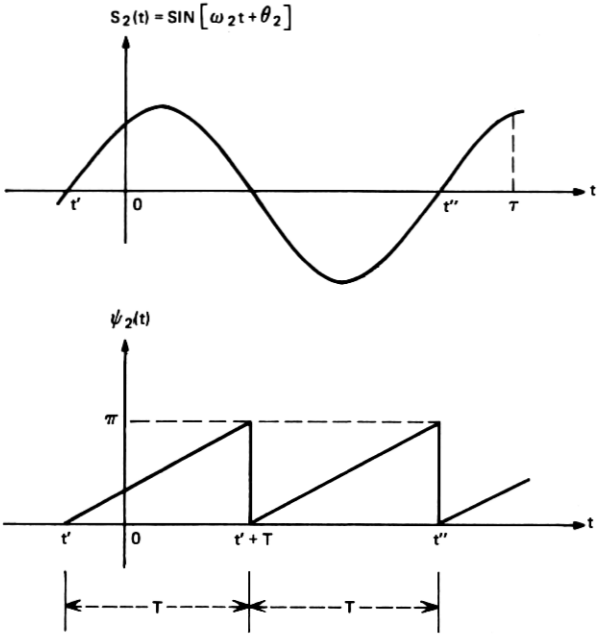

Fig. 3—Illustration of $S_2(t)$, $N_2(t)$, and $\psi_2(t)$.

at $t = 0$. Without loss of generality, we may assume $0 \leqq \theta_1 \leqq \pi$, and $0 \leqq \theta_2 \leqq \pi$.

Let us derive an analytic expression for the number of zero crossings of $s_2(t)$ from $t = 0$ to a particular time instant τ. As illustrated in Fig. 3, t' is the time instant at which the last zero crossing prior to $t = 0$ takes place, and t'' is the time instant at which the last zero crossing prior to $t = \tau$ takes place. It is obvious from Fig. 3 that the number of zero crossings in the time interval 0 to τ is

$$N_2(\tau) = \frac{\omega_2 t'' + \theta_2}{\pi}. \tag{3}$$

Note from (3) that the phase cumulated from t'' to τ does not contribute to the value of $N_2(\tau)$. This residual phase (or phase quantization error) will be designated $\psi_2(\tau)$, i.e.,

$$\psi_2(\tau) = \omega_2 \tau - \omega_2 t''. \tag{4}$$

Equations (3) and (4) hold for all $\tau > 0$; therefore, we can replace their τ by the time variable t. The variation of $\psi_2(t)$ with t is illustrated in

Fig. 3. Note that $\psi_2(t)$ increases from 0 to π. When $\psi_2(t)$ reaches π radians, a zero crossing takes place; and $\psi_2(t)$ drops to zero and increases from zero again. Clearly, $0 \leqq \psi_2(t) \leqq \pi$. Since $s_2(t)$ is a pure sine wave, $\psi_2(t)$ is a sawtooth wave.

From (3) and (4), we have

$$N_2(t) = \frac{\omega_2 t + \theta_2 - \psi_2(t)}{\pi}. \tag{5}$$

Similarly, one can write the number of zero crossings of $s_1(t)$ as

$$N_1(t) = \frac{\omega_1 t + \alpha_1 \int_0^t v_1(\tau)\, d\tau + \theta_1 - \psi_1(t)}{\pi} \tag{6}$$

where $\psi_1(t)$ is the residual phase as illustrated in Fig. 4. As can be seen, $0 \leqq \psi_1(t) \leqq \pi$. Note that $\psi_1(t)$ is not shown as a sawtooth wave in Fig. 4 because $s_1(t)$ is not a pure sine wave in the transient stage after $t = 0$.

In this paper, the filter $F(s)$ in Fig. 2 is assumed to be the usual RC filter (Fig. 5). Thus, its transfer function $F(s)$ is $1/(1 + sCR)$. Substituting (5) and (6) into (1), and rearranging the equation, we obtain

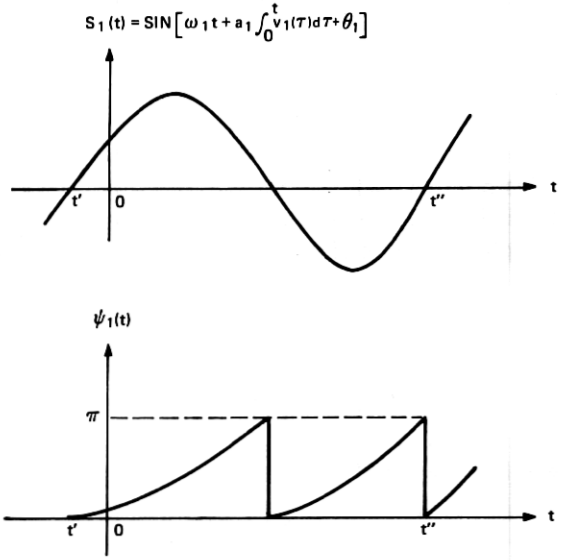

Fig. 4—Illustration of $S_1(t)$, $N_1(t)$, and $\psi_1(t)$.

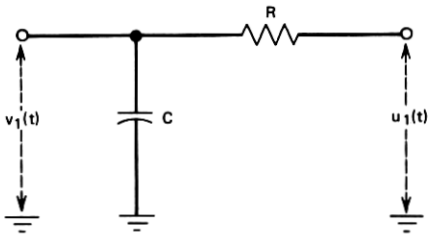

Fig. 5—*RC* filter in the rate-locked loop.

$$u_1(t) = k\left[\delta t - \alpha_1 \int_0^t v_1(\tau)\, d\tau + \theta_2 - \theta_1 + \psi_1(t) - \psi_2(t)\right] \tag{7}$$

where

$$k = \frac{e_1}{\pi} \tag{8}$$

$$\delta = \omega_2 - \omega_1 \,. \tag{9}$$

We shall use one-sided Laplace transform in the analysis (the words one-sided will be omitted). As usual, the Laplace transform of a time function will be consistently denoted by the appropriate capital letter. For instance, $U_1(s)$ will denote the Laplace transform of $u_1(t)$. The symbol $\mathsf{L}[f(t)]$ denotes the Laplace transform of $f(t)$, and the symbol $\mathsf{L}^{-1}[F(s)]$ denotes the inverse Laplace transform of $F(s)$. Taking the Laplace transform of (7), we obtain

$$U_1(s) = k\left[\frac{\delta}{s^2} - \alpha_1 \frac{V_1(s)}{s} + \frac{\theta_2}{s} - \frac{\theta_1}{s} + \Psi_1(s) - \Psi_2(s)\right]. \tag{10}$$

Multiplying both sides of (10) by $F(s)$, using $F(s)U_1(s) = V_1(s)$, and rewriting the resulting equation in time domain we obtain

$$\begin{aligned} v_1(t) = {} & \mathsf{L}^{-1}\left[H(s)\frac{\delta}{s^2}\right] + \mathsf{L}^{-1}\left[H(s)\frac{\theta_2}{s}\right] - \mathsf{L}^{-1}\left[H(s)\frac{\theta_1}{s}\right] \\ & - \mathsf{L}^{-1}[H(s)\Psi_2(s)] + \mathsf{L}^{-1}[H(s)\Psi_1(s)], \qquad t > 0 \end{aligned} \tag{11}$$

where

$$H(s) = \frac{ks}{CR(s + r_1)(s + r_2)}$$

$$r_1 = \frac{1 + \sqrt{1 - 4CRk\alpha_1}}{2CR}$$

$$r_2 = \frac{1 - \sqrt{1 - 4CRk\alpha_1}}{2CR}.$$

The two roots r_1 and r_2 are real numbers when $1 - 4CRk\alpha_1 > 0$, and are complex numbers when $1 - 4CRk\alpha_1 < 0$. It can be shown that in the second case the frequency of $s_1(t)$ overshoots that of $s_2(t)$ before it finally settles. Such an overshooting should be avoided because Station 1 may be required to operate in the slave-to-slave mode (see Section V). Therefore, throughout this paper we assume

$$1 - 4CRk\alpha_1 > 0. \tag{12}$$

III. STEADY-STATE AND TRANSIENT ANALYSES

In the master-to-slave mode, we have to consider the following questions:

(*i*) Can the signaling rate of Station 1 lock to that of Station 2 in the presence of phase quantization errors?
(*ii*) What is the steady-state frequency of VCO_1 ?
(*iii*) During the transient stage after $t = 0$, the signaling rate of Station 1 can be higher than that of Station 2. Therefore, data can be transmitted from Station 1 to Station 2 faster than it can be transmitted out of Station 2. Consequently, a buffer storage is required at Station 2. What should be the size of this buffer?
(*iv*) The digital phase detector is a counter that counts the difference between the number of zero crossings of $s_1(t)$ and $s_2(t)$. How many stages are required in the counter to avoid overflow (i.e., to ensure pulling in)?

We shall first determine the transient response of the system in Section 3.1, and then consider these questions in Sections 3.2 to 3.4.

3.1 *Transient Response and Settling Time*

We evaluate the first three inverse transforms in (11) to obtain

$$\mathcal{L}^{-1}\left[H(s)\frac{\delta}{s^2}\right] = \frac{k\delta}{CRr_1r_2(r_1 - r_2)}\left[(r_1 - r_2) + r_2e^{-r_1t} - r_1e^{-r_2t}\right] \tag{13}$$

$$\mathcal{L}^{-1}\left[H(s)\frac{\theta_2}{s}\right] - \mathcal{L}^{-1}\left[H(s)\frac{\theta_1}{s}\right] = \frac{(\theta_2 - \theta_1)k}{CR(r_1 - r_2)}[e^{-r_2 t} - e^{-r_1 t}]. \quad (14)$$

The fourth inverse transform $\mathcal{L}^{-1}[H(s)\Psi_2(s)]$ is more difficult to evaluate. We obtain after lengthy manipulations

$$\mathcal{L}^{-1}[H(s)\Psi_2(s)] = a(t) + p(t) \quad (15)$$

where

$$a(t) = \frac{k}{\sqrt{1 - 4CRk\alpha_1}}\left[\frac{\omega_2}{r_1} - \theta_2 + \frac{\pi e^{r_1 t_5}}{1 - e^{r_1 T}}\right]e^{-r_1 t} + \frac{k}{\sqrt{1 - 4CRk\alpha_1}}\left[-\frac{\omega_2}{r_2} + \theta_2 - \frac{\pi e^{r_2 t_5}}{1 - e^{r_2 T}}\right]e^{-r_2 t}. \quad (16)$$

$p(t)$ = a periodic function of period T, identical with $p_0(t)$ in the time period $0 \leqq t \leqq T$ (17)

$$p_0(t) = \frac{\omega_2}{\alpha_1} + \frac{k\pi e^{r_1 t_5}}{\sqrt{1 - 4CRk\alpha_1}\,(1 - e^{r_1 T})}[-1 + (1 - e^{r_1 T})u(t - t_5)]e^{-r_1 t} + \frac{k\pi e^{r_2 t_5}}{\sqrt{1 - 4CRk\alpha_1}\,(1 - e^{r_2 T})}[1 - (1 - e^{r_2 T})u(t - t_5)]e^{-r_2 t}. \quad (18)$$

Note that $a(t)$ is the sum of two decaying exponential terms. When t increases, $a(t)$ approaches zero, and only the periodic steady-state response $p(t)$ remains. It can be shown that $p(t)$ has zero mean.

Now consider the last inverse transform $\mathcal{L}^{-1}[H(s)\Psi_1(s)]$ in (11). Since $\Psi_1(s)$ is the Laplace transform of $\psi_1(t)$, $\mathcal{L}^{-1}[H(s)\Psi_1(s)]$ can be evaluated if $\psi_1(t)$ can be determined. As illustrated in Fig. 4, $\psi_1(t)$ depends on the positions of the zero crossings of $s_1(t)$. Furthermore, because we are dealing with a closed-loop control system, $\psi_1(t)$ and the phase of $s_1(t)$ must satisfy the integral equation (7). In order to determine $\psi_1(t)$, one must simultaneously consider (7) and the zero crossings of $s_1(t)$. The mathematical problem is extremely complex and it is impossible to obtain a closed-form expression of $\psi_1(t)$ for all t. Consequently, the inverse transform $\mathcal{L}^{-1}[H(s)\Psi_1(s)]$ cannot be evaluated in closed form. However, we have obtained a tight upper and lower bound for its value as follows:

$$|\mathcal{L}^{-1}[H(s)\Psi_1(s)]| < 2e_1 . \quad (19)$$

We have obtained the closed-form expression of the first four components of $v_1(t)$, and tightly bounded the fifth component of $v_1(t)$. This gives the transient response of the system. Note from (13) to (19) that transients in $v_1(t)$ either decay exponentially or can be bounded by a small number. Thus, the system is well behaved in the transient stage. Furthermore, from these equations, one can plot $v_1(t)$ vs t, and easily estimate the settling time of VCO_1 . The settling time of VCO_1 can be rather long when CR is large. For example, consider the first term $\mathcal{L}^{-1}[H(s)\delta/s^2]$ in $v_1(t)$ (this is usually the dominating term in $v_1(t)$). From (13) it can be rewritten as

$$\mathcal{L}^{-1}\left[H(s)\frac{\delta}{s^2}\right] = \frac{\delta}{\alpha_1}\left[1 - e^{-r_1 t} + \frac{r_1(e^{-r_2 t} - e^{-r_1 t})}{r_2 - r_1}\right].$$

Since $r_1 > r_2 > 0$, the last term in the right-side bracket is negative for all t. Thus, the convergence of $\mathcal{L}^{-1}[H(s)\delta/s^2]$ is even slower than the convergence of the time function $1 - e^{-r_1 t}$. This clearly shows that $v_1(t)$ converges slowly when the filter time constant CR is large.

3.2 *Steady-State Frequency of VCO_1*

Now we answer the first two questions at the beginning of Section III. First, we have found that the signaling rate of Station 1 will lock to that of Station 2 in the presence of phase quantization errors. The proof of this is complicated, and is given in the Appendix. In this section, we examine the steady-state frequency of VCO_1 , and point out an important difference between digital and analog phase detectors. The instantaneous frequency of VCO_1 is $[\omega_1 + \alpha_1 v_1(t)/2\pi]$. In order to see if it approaches a fixed steady-state value, we evaluate $\lim_{t\to\infty} v_1(t)$, which can be found by evaluating the limits of the five inverse transforms in (11). As shown in the Appendix, when signaling rate of Station 1 locks to that of Station 2, the zero crossings of $s_1(t)$ and $s_2(t)$ will alternate with probability one, and $\psi_1(t)$ will be a periodic function of period T. This means that $\mathcal{L}^{-1}[H(s)\psi_1(s)]$ also approaches a periodic function of period T. Let this periodic function be denoted by $q(t)$. Then, one can show from (11) that

$$\begin{pmatrix}\text{Instantaneous fre-}\\ \text{quency of VCO}_1\end{pmatrix} = f_2 - \frac{\alpha_1}{2\pi}p(t) + \frac{\alpha_1}{2\pi}q(t). \tag{20}$$

When signaling rate of Station 1 locks to that of Station 2, zero crossings of $s_1(t)$ and $s_2(t)$ alternate. Therefore, $\psi_1(t) \neq \psi_2(t)$ and $p(t) \neq q(t)$. Thus, from (20), instantaneous frequency of VCO_1 does

not lock to the master clock frequency f_2 . Instead, it is a periodic function $f_2 - (\alpha_1/2\pi)p(t) + (\alpha_1/2\pi)q(t)$. The output $s_1(t)$ of VCO_1 is a periodic wave with the same period as $s_2(t)$; however, it is not a pure sine wave as one would expect from experience with analog-phase lock loops. *The digital loop locks to neither the instantaneous frequency nor the phase of the incoming signal* $s_2(t)$. *It locks only to the rate of zero crossings of* $s_2(t)$. For this reason, it should be referred to as a digital rate-locked loop, rather than a digital frequency-locked loop or a digital phase-locked loop. This difference between digital and analog loops should be noted in the applications.

3.3 *Size of the Data Buffer at Station 2*

As described in Section II, Station 2 transmits to Station 1 at a standard rate of f_2 digits per second. In general, Station 1 is also required to transmit to Station 2 at this standard rate. To achieve this, Station 1 transmits a digit to Station 2 at every second zero crossing of $s_1(t)$ [this enables station 1 to transmit also at the standard rate when $s_1(t)$ is synchronized to $s_2(t)$].

Usually, Station 2 relays the data it receives from Station 1 to another station at the standard rate of f_2 digits per second. Thus, when the system is in synchronization, data is transmitted to Station 2 at the same rate as it is transmitted out of Station 2. However, when Station 1 is first synchronized (that is, during the transient stage of synchronization), the transmission rate of Station 1 can be higher than f_2 . Consequently, during the transient stage, data can be transmitted from Station 1 to Station 2 faster than it can be transmitted out of Station 2. This means a data buffer is required at Station 2. In this section, we determine the size of this buffer.

As defined in Section II, $N_1(t)$ is the number of zero crossings of $s_1(t)$ in the time interval 0 to t. Since Station 1 transmits a digit to station 2 at every second zero crossing of $s_1(t)$, the number of digits transmitted from Station 1 to Station 2 in the time interval 0 to t is $N_1(t)/2$ or $N_1(t) - 1/2$, depending on whether $N_1(t)$ is even or odd. To simplify our discussions, we shall use the following definition throughout this paper.

Definition: For any positive number a, $\langle a \rangle$ denotes the integer immediately less than a when a is not an integer. $\langle a \rangle = a$ when a is an integer.

Using this definition, the number of digits transmitted from Station 1 to Station 2 in the time interval 0 to t is $\langle N_1(t)/2 \rangle$. The number of digits Station 1 should transmit in this time interval is $\langle N_2(t)/2 \rangle$. If

$\langle N_1(t)/2\rangle$ is larger than $\langle N_2(t)/2\rangle$, a buffer would be required at Station 2 and the buffer size is $\langle N_1(t)/2\rangle - \langle N_2(t)/2\rangle$ digits. It can be shown from the previous equations that

$$-\left[\frac{\omega'}{e_1\alpha_1} + 3\right] < N_1(t) - N_2(t) < \frac{\omega'}{e_1\alpha_1} + 3. \tag{21}$$

Since the buffer size is $\langle N_1(t)/2\rangle - \langle N_2(t)/2\rangle$, we obtain from (21)

$$\text{Buffer Size} < \frac{\omega'}{2e_1\alpha_1} + 2. \tag{22}$$

Equation (22) gives an upper bound for the buffer size. It can also be shown that in order to prevent overflow the buffer size must be greater than $(\omega'/2e_1\alpha_1) - \frac{1}{2}$. Combining this with (22), we have

$$\frac{\omega'}{2e_1\alpha_1} - \tfrac{1}{2} < \text{Buffer Size} < \frac{\omega'}{2e_1\alpha_1} + 2. \tag{23}$$

Let us define $B = \langle \omega'/2e_1\alpha_1 + 2\rangle$. It can be seen from (23) that the buffer size is B, $B - 1$, or $B - 2$. Thus, the buffer size is determined to within two digits. Since the two-digit difference is negligible, one may use the simple formula

$$\text{Buffer Size} = B = \left\langle \frac{\omega'}{2e_1\alpha_1} + 2 \right\rangle \text{digits}. \tag{24}$$

As explained at the end of Section II, in this paper we use the constraint $1 - 4CRk\alpha_1 > 0$. From this constraint, we can rewrite (24) as

$$\text{Buffer Size} = \left\langle \frac{2CR\omega'}{\beta_1\pi} + 2 \right\rangle \text{digits} \tag{25}$$

where $\beta_1 = 4CRe_1\alpha_1/\pi$. Clearly, $0 < \beta_1 < 1$. Equation (25) will be used in later discussions.

3.4 *Counter Size of the Digital Phase Detector*

The counter in the digital phase detector counts the difference between $N_2(t)$ and $N_1(t)$. Now we determine the counter size so that the counter will not overflow when the maximum positive count or negative count is reached. Consider first the case of negative counts. It can be shown that $N_1(t) - N_2(t)$ can be larger than $\omega'/e_1\alpha_1$. It has been shown in the preceding subsection that $N_1(t) - N_2(t)$ must be less than $\omega'/e_1\alpha_1 + 3$. Thus, if we define

$$N = \left\langle \frac{\omega'}{e_1\alpha_1} + 3 \right\rangle = \left\langle \frac{4CR\omega'}{\beta_1\pi} + 3 \right\rangle,$$

the integer $N_1(t) - N_2(t)$ can be as large as $N - 2$, but will not exceed N. Therefore, the counter will not overflow if it can count $N_1(t) - N_2(t)$ up to $N_1(t) - N_2(t) = N$.

Next, consider positive counts. One can show that the counter will not overflow if it can count $N_2(t) - N_1(t)$ up to $N_2(t) - N_1(t) = N$. Combining the two cases, we see that the counter will not overflow if

$$\text{Counter Size} = \pm N \text{ counts} = \pm\left\langle \frac{4CR\omega'}{\beta_1\pi} + 3 \right\rangle \text{counts} \qquad (26)$$

where β_1 is defined after (25).

IV. SLAVE-TO-SLAVE SYNCHRONIZATION USING DIGITAL RATE-LOCKED LOOPS

In this section, we consider mutual synchronization between two data stations where each station regards the clock at the other station as the master clock. Such a mutual synchronization is usually called slave-to-slave synchronization.

A mathematical model of slave-to-slave synchronization is depicted in Fig. 6. The local oscillator at Station 1 (VCO_1 in Fig. 6) emits a timing signal $S_{11}(t)$ which controls the transmission of data from

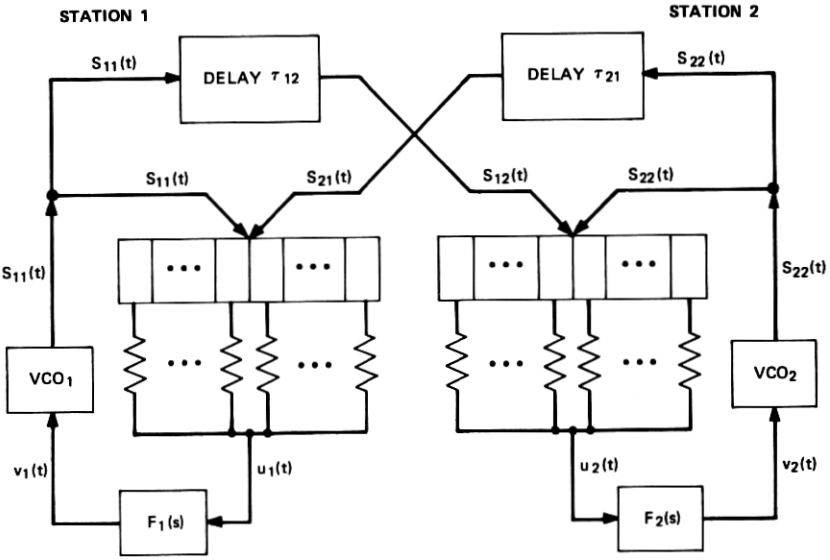

Fig. 6—Slave-to-slave synchronization with digital rate-locked loops at both stations.

Station 1 to Station 2. [For example, Station 1 may transmit a digit to Station 2 at every second zero crossing of $S_{11}(t)$.] Station 2 derives from the received data a timing signal $S_{12}(t)$ and compares $S_{12}(t)$ with its local oscillator output $S_{22}(t)$ at the digital phase detector. The digital phase detector is essentially a counter which counts the zero crossings of $S_{12}(t)$ and $S_{22}(t)$ and produces an error signal $u_2(t)$ proportional to the difference between these two counts. The error signal $u_2(t)$ is passed through a filter $F_2(s)$ to control the frequency of VCO_2. Thus, in this fashion, Station 2 adjusts its clock rate toward that of Station 1. Similarly, as depicted in Figure 6, Station 1 regards the clock at Station 2 as the master clock and adjusts its clock rate toward that of Station 2.

Practically, it is impossible to activate the two counters at the two different stations at the same time instant. Therefore, in this study, we consider an arbitrary starting sequence as follows:

(*i*) At an arbitrary time instant t_1, either the counter at Station 1 or the counter at Station 2 is activated.
(*ii*) The other counter is activated at an arbitrary later time instant $t_2 (t_2 > t_1)$.

For analytical purpose, we shift the time origin such that $t_2 = 0$. We shall analyze the behavior of the system for $t > 0$.

Let ω_1 be the free-running radian frequency of VCO_1, then we can write

$$\begin{aligned} s_{11}(t) &= \sin \rho_{11}(t) \\ &= \sin \left[\omega_1 t + \alpha_1 \int_0^t v_1(\tau)\, d\tau + \theta_{11} \right] \end{aligned} \tag{27}$$

and

$$s_{12}(t) = \sin [\rho_{11}(t - \tau_{12})] \tag{28}$$

where τ_{12} is the time delay introduced by the channel. Similarly, the free-running frequency of VCO_2 is denoted ω_2 and

$$\begin{aligned} s_{22}(t) &= \sin \rho_{22}(t) \\ &= \sin \left[\omega_2 t + \alpha_2 \int_0^t v_2(\tau)\, d\tau + \theta_{22} \right] \end{aligned} \tag{29}$$

and

$$s_{21}(t) = \sin [\rho_{22}(t - \tau_{21})]. \tag{30}$$

We define $N_{ij}(t)$ as the number of counts from $s_{ij}(t)$ in the time interval 0 to t. Let us first derive an analytical expression for $N_{11}(t)$. From (27), we can write

$$\omega_1 t + \alpha_1 \int_0^t v_1(\tau)\, d\tau + \theta_{11} = M\pi N_{11}(t) + \psi_{11}(t) \tag{31}$$

where the parameter M is defined by: M equals one when the counters at the two stations count both the upward and downward zero crossings; M equals two when the counters count only the upward (or downward) zero crossings. The last term $\psi_{11}(t)$ in the above equation represents phase quantization errors and $0 \leqq \psi_{11}(t) < M\pi$. From the above equation we have

$$N_{11}(t) = \frac{1}{M\pi}\left[\omega_1 t + \alpha_1 \int_0^t v_1(\tau)\, d\tau + \theta_{11} - \psi_{11}(t)\right]. \tag{32}$$

Similarly, one can write analytical expressions for $N_{12}(t)$, $N_{21}(t)$, and $N_{22}(t)$.

At Station 1, the digital counter output is

$$u_1(t) = u_1(0) + e_1[N_{21}(t) - N_{11}(t)] \tag{33}$$

where $u_1(0)$ is the initial count at $t = 0$. Let us define

$$k_1 = \frac{e_1}{M\pi} \tag{34}$$

$$\delta = \omega_2 - \omega_1 \tag{35}$$

$$\theta_1 = \theta_{21} - \theta_{11} \tag{36}$$

$$R_{21}(s) = e^{-s\tau_{21}} \int_{-\tau_{21}}^{0} v_2(t) e^{-st}\, dt. \tag{37}$$

The filters $F_1(s)$ and $F_2(s)$ in Fig. 6 are assumed to be the usual RC filters, i.e.,

$$F_1(s) = \frac{1}{1 + sC_1R_1} \tag{38}$$

$$F_2(s) = \frac{1}{1 + sC_2R_2}. \tag{39}$$

At Station 2, the digital filter output is

$$u_2(t) = u_2(0) + e_2[N_{12}(t) - N_{22}(t)] \tag{40}$$

where $u_2(0)$ is the initial count at $t = 0$. Furthermore, we define

$$k_2 = \frac{e_2}{M\pi} \tag{41}$$

$$\theta_2 = \theta_{12} - \theta_{22} \tag{42}$$

$$R_{12}(s) = e^{-s\tau_{12}} \int_{-\tau_{12}}^{0} v_1(t)e^{-st}\, dt. \tag{43}$$

From the previous equations, we can determine $V_1(s)$ and $V_2(s)$. The results are:

$$V_1(s) = \frac{A_1(s)}{B(s)} + \frac{A_2(s)}{B(s)} + \frac{A_3(s)}{B(s)} + \frac{A_4(s)}{B(s)} + \frac{A_5(s)}{B(s)} \tag{44}$$

where

$$A_1(s) = \left[\frac{u_1(0)F_1(s)}{s} + \frac{k_1\theta_1F_1(s)}{s} + v_1(0)C_1R_1F_1(s) + \frac{k_1\alpha_2R_{21}(s)F_1(s)}{s}\right] \cdot \left[1 + k_2\alpha_2\frac{F_2(s)}{s}\right]$$

$$A_2(s) = [-k_1\Psi_{21}(s)F_1(s) + k_1\Psi_{11}(s)F_1(s)]\left[1 + k_2\alpha_2\frac{F_2(s)}{s}\right]$$

$$A_3(s) = \left[\frac{u_2(0)F_2(s)}{s} + \frac{k_2\theta_2F_2(s)}{s} + v_2(0)C_2R_2F_2(s) + \frac{k_2\alpha_1R_{12}(s)F_2(s)}{s}\right] \cdot \left[k_1\alpha_2\frac{e^{-s\tau_{21}}}{s}F_1(s)\right]$$

$$A_4(s) = [-k_2\Psi_{12}(s)F_2(s) + k_2\Psi_{22}(s)F_2(s)]\left[k_1\alpha_2\frac{e^{-s\tau_{21}}}{s}F_1(s)\right]$$

$$A_5(s) = k_1\,\delta\frac{F_1(s)}{s^2}\left[1 + k_2\alpha_2\frac{F_2(s)}{s}(1 - e^{-s\tau_{21}})\right]$$

$$B(s) = 1 + k_1\alpha_1\frac{F_1(s)}{s} + k_2\alpha_2\frac{F_2(s)}{s} + k_1\alpha_1k_2\alpha_2\frac{F_1(s)}{s}\frac{F_2(s)}{s}[1 - e^{-s(\tau_{12}+\tau_{21})}].$$

Similarly, we obtain

$$V_2(s) = \frac{A_6(s)}{B(s)} + \frac{A_7(s)}{B(s)} + \frac{A_8(s)}{B(s)} + \frac{A_9(s)}{B(s)} + \frac{A_{10}(s)}{B(s)} \tag{45}$$

where

$$A_6(s) = \left[\frac{u_2(0)F_2(s)}{s} + \frac{k_2\theta_2F_2(s)}{s} + v_2(0)C_2R_2F_2(s) + \frac{k_2\alpha_1R_{12}(s)F_2(s)}{s}\right] \cdot \left[1 + k_1\alpha_1\frac{F_1(s)}{s}\right]$$

$$A_7(s) = [-k_2\Psi_{12}(s)F_2(s) + k_2\Psi_{22}(s)F_2(s)]\left[1 + k_1\alpha_1\frac{F_1(s)}{s}\right]$$

$$A_8(s) = \left[\frac{u_1(0)F_1(s)}{s} + \frac{k_1\theta_1F_1(s)}{s} + v_1(0)C_1R_1F_1(s) + \frac{k_1\alpha_2R_{21}(s)F_1(s)}{s}\right] \cdot \left[k_2\alpha_1e^{-s\tau_{12}}\frac{F_2(s)}{s}\right]$$

$$A_9(s) = [-k_1\Psi_{21}(s)F_1(s) + k_1\Psi_{11}(s)F_1(s)]\left[k_2\alpha_1e^{-s\tau_{12}}\frac{F_2(s)}{s}\right]$$

$$A_{10}(s) = -k_2\,\delta\frac{F_2(s)}{s^2}\left[1 + k_1\alpha_1\frac{F_1(s)}{s}(1 - e^{-s\tau_{12}})\right]$$

Note that our problem is not solved. Equation (44) is not a closed-form solution of $V_1(s)$ because $\Psi_{ij}(s)$, which appears in $A_2(s)$ and $A_4(s)$, depends on $V_1(s)$ and $V_2(s)$ (the phase quantization errors $\psi_{ij}(t)$ depends on $v_1(t)$ and $v_2(t)$). Similarly, (45) is not a closed-form solution of $V_2(s)$. These equations will, however, enable us to examine the steady-state behavior of the system in the following sections.

4.1 *A Steady-State Solution of Signaling Rates*

As described previously, the zero crossings of $s_{11}(t)$ are used to control the transmission from Station 1 to Station 2 (for example, Station 1 may transmit a digit to Station 2 at every second zero crossing of $s_{11}(t)$). Similarly, the zero crossings of $s_{22}(t)$ are used to control the transmission from Station 2 to Station 1. Therefore, to determine the steady-state signaling rates of these two stations, it suffices to determine the steady-state distribution of the zero crossings of $s_{11}(t)$ and $s_{22}(t)$. To facilitate our discussion, let us first introduce the following definition.

Definition: $s_0(t)$ denotes a sine wave $\sin \omega_0 t$ with

$$\omega_0 = \frac{1}{k_1\alpha_1 + k_2\alpha_2 + k_1\alpha_1k_2\alpha_2(\tau_{12} + \tau_{21})}[\omega_1k_2\alpha_2 + \omega_2k_1\alpha_1 + \omega_1k_1\alpha_1k_2\alpha_2\tau_{12} + \omega_2k_1\alpha_1k_2\alpha_2\tau_{21} + [u_1(0) + k_1\theta_1 + k_1\alpha_2R_{21}(0)]k_2\alpha_1\alpha_2 + [u_2(0) + k_2\theta_2 + k_2\alpha_1R_{12}(0)]k_1\alpha_1\alpha_2]. \quad (46)$$

Based on (44) and (45), a steady-state solution of the zero-crossing distribution has been obtained.[10] In order to conserve space, let us omit the lengthy derivations and write only the results as follows: *A Steady-State Solution:* When the counters at the two stations count both the upward and downward zero crossings of $s_{ij}(t)$, $i, j = 1, 2$, the upward and downward zero crossings of $s_{ij}(t)$, $i, j = 1, 2$, are uniformly spaced when $t \to \infty$ and the time interval between each two consecutive zero crossings of $s_{ij}(t)$, $i, j = 1, 2$, is identical with the time interval between each two consecutive zero crossings of $s_0(t)$.

If the counters count only the upward (or downward) zero crossings, the above solution should be modified: When the counters at the two stations count only the upward (or downward) zero crossings of $s_{ij}(t)$, $i, j = 1, 2$, the upward (or downward) zero crossings of $s_{ij}(t)$, $i, j = 1, 2$, are uniformly spaced when $t \to \infty$, and the time interval between each two consecutive upward (or downward) zero crossings of $s_{ij}(t)$, $i, j = 1, 2$, is identical with the time interval between each two consecutive upward (or downward) zero crossings of $s_0(t)$.

4.2 *Analysis of the Steady-State Signaling Rate*

In this section, we show that the system can be easily designed such that the steady-state signaling rate lies within desired limits.

Before the two stations are mutually synchronized, $s_{11}(t)$ is $\sin \omega_1 t$ and the signaling rate of Station 1 is $h\omega_1$ digits/second. (h is a proportionality constant. For example, $h = 1/2\pi$ when Station 1 transmits a digit at every second zero crossing of $s_{11}(t)$.) Similarly, before the two stations are synchronized, $s_{22}(t)$ is $\sin \omega_2 t$ and the signaling rate of Station 2 is $h\omega_2$ digits/second. When the two stations are mutually synchronized, $s_{11}(t)$ and $s_{22}(t)$ have the same zero-crossing distribution as $s_o(t) = \sin \omega_o t$ and the signaling rates of the two stations are $h\omega_o$ digits/second. The synchronization is satisfactory if $h\omega_o$ is sufficiently close to $h\omega_1$ or $h\omega_2$. More specifically, the steady-state signaling rate is satisfactory if

$$h\omega_1 - \epsilon < h\omega_0 < h\omega_2 + \epsilon \tag{47}$$

when $\omega_1 < \omega_2$, and if

$$h\omega_2 - \epsilon < h\omega_0 < h\omega_1 + \epsilon \tag{48}$$

when $\omega_2 < \omega_1$. The number ϵ is a prescribed small number.

As can be seen from (46), ω_o depends on ω_1, ω_2, and the following parameters: gains e_1 and e_2 of the two counters, gains α_1 and α_2 of the two oscillators, initial counter outputs $u_1(0)$ and $u_2(0)$, initial phases

θ_1 and θ_2, initial filter outputs $v_1(t)$ and $v_2(t)$, and the time delays τ_{12} and τ_{21} in the communication channels. Since ω_o depends on so many parameters, it is not immediately clear whether ω_o satisfies the specifications in (47) and (48). In the following, we derive simple design constraints such that when these constraints are satisfied, ω_o will satisfy the specifications in (47) and (48).

So far, we have considered the arbitrary starting sequence described at the beginning of this section. Since we may always designate the station that is started first as Station 1, we need to consider only the following starting sequence in the sequel: At an arbitrary time $t_1 < 0$, the counter at Station 1 is activated. The counter at Station 2 is activated at $t = 0$.

There are two cases to be considered: $\omega_1 \leqq \omega_2$ and $\omega_1 > \omega_2$. Our analyses of these two cases yield the same design constraint; hence, we describe only the case $\omega_1 \leqq \omega_2$.

Note from the starting sequence that for $t \leqq 0$, Station 2 is the master and Station 1 is the slave. We therefore can use the results in Section III to bound $v_1(t)$ for $t \leqq 0$. From this, we can show that ω_o always satisfies the following inequalities:

$$\omega_0 > \left[\omega_1 + \frac{(k_1\alpha_1 + k_1\alpha_1k_2\alpha_2\tau_{21})(\omega_2 - \omega_1)}{k_1\alpha_1 + k_2\alpha_2 + k_1\alpha_1k_2\alpha_2(\tau_{12} + \tau_{21})} - \frac{[\frac{5}{6}k_2\alpha_2 + k_1\alpha_1k_2\alpha_2\tau_{12}]6e_1\alpha_1}{k_1\alpha_1 + k_2\alpha_2 + k_1\alpha_1k_2\alpha_2(\tau_{12} + \tau_{21})}\right] \tag{49}$$

and

$$\omega_0 < \omega_2 + \frac{[\frac{5}{6}k_2\alpha_2 + k_1\alpha_1k_2\alpha_2\tau_{12}]6e_1\alpha_1}{k_1\alpha_1 + k_2\alpha_2 + k_1\alpha_1k_2\alpha_2(\tau_{12} + \tau_{21})}. \tag{50}$$

It should be clear from (49) and (50) that, regardless of the values of the time delays τ_{12} and τ_{21}, one can easily select the gain $e_1\alpha_1$ of the first station so that ω_o will satisfy the constraint in (47). To show this more explicitly, we further simplify (49) and (50) (this simplification will, however, make the constraint on $e_1\alpha_1$ slightly more stringent). Since ω_o satisfies (49) and (50), ω_o will definitely lie in the following broader range

$$\omega_1 - 6e_1\alpha_1 < \omega_0 < \omega_2 + 6e_1\alpha_1. \tag{51}$$

Comparing (51) with (47) shows that ω_o satisfies the specification in (47) if

$$e_1\alpha_1 < \frac{\epsilon}{6h}. \tag{52}$$

From (52), one can easily determine the value of $e_1\alpha_1$. Since we have designated the station that is started first as Station 1, and since either station can be started first, (52) should be applied to both stations. To emphasize this, we replace (52) with the following two constraints

$$e_1\alpha_1 < \frac{\epsilon}{6h} \tag{53}$$

$$e_2\alpha_2 < \frac{\epsilon}{6h}. \tag{54}$$

Now, to summarize this section: we have shown that if the gains of the two stations are designed to satisfy the simple constraints in (53) and (54), ω_o will satisfy (47) and the steady-state signaling rates will be satisfactory. Since (53) and (54) can be easily satisfied, and are independent of all the other parameters in (46), we conclude that the steady-state signaling rate can be easily made satisfactory regardless of the starting sequence, the initial system conditions, and the time delays in the communication channels.

V. SUMMARY AND CONCLUSIONS

Sections II and III examine the behavior of the system in the master-to-slave mode. The station with the slave clock (Station 1 in Fig. 1) represents a data station, while the station with the master clock (Station 2) represents a station in the digital transmission facility. The slave clock at Station 1 employs a digital rate-locked loop which consists of a digital counter, an *RC* filter, and a slave oscillator (Fig. 2). The counter is not restricted to have only one stage. A mathematical model of the system is formulated in Section II. Transient response of the system is determined in Section 3.1. It is shown that, under the condition $1 - 4CRk\alpha_1 > 0$ in (12), the signaling rate of Station 1 approaches that of Station 2 in a monotone fashion (transients either decay exponentially as shown in (13), (14), (15) and (16), or can be tightly bounded as shown in (19)).

From the transient response, settling time of the slave oscillator can be easily estimated. As discussed at the end of Section 3.1, this settling time can be rather long when the *RC* filter has a large time constant. For fast start-up purpose, it may be desirable for Station 1 to transmit data before the slave oscillator is completely settled. Thus, during the start-up period, data can be transmitted from Station 1 to Station 2 faster than it can be transmitted out of Station 2. Con-

sequently, a buffer storage is required at Station 2. This buffer size is determined and is given in (25). Section 3.4 examines the size of the counter in the rate-locked loop (counter size determines the pull-in range of the rate-locked loop). In order to avoid counter overflow (that is, to ensure pulling in), the counter must have a certain minimum size. This minimum size is determined and is given in (26).

As emphasized in Section 3.2, the slave oscillator in the rate-locked loop locks to neither the instantaneous frequency nor the phase of the master oscillator. It locks only to the rate of zero crossings of the master oscillator. For this reason, we refer to this control loop as a rate-locked loop, instead of a frequency-locked loop or a phase-locked loop. This difference, while immaterial in the present application, should be carefully noted in other applications.

Section IV examines the behavior of the system in the slave-to-slave mode. The two stations to be mutually synchronized represent two data stations connected by analog transmission facilities. A rate-locked loop is used at each station, and an *RC* filter is included in each loop. A random starting sequence is considered where either station can be started first, with the other station activated at an arbitrary later time. When the two stations are mutually synchronized, the two stations settle to the same steady-state signaling rate $h\omega_o$ (h is a proportionality constant and ω_o is given in (46)). Equation (46) shows that ω_o depends on the gains of the counters and oscillators, the initial conditions of the counters, filters, and oscillators, and the time delays in the communication channels. It is shown that, although ω_o depends on so many parameters, the steady-state signaling rate $h\omega_o$ will lie within desired limits if the simple design constraints in (53) and (54) are satisfied (these conditions can be relaxed by using the more complicated equations (49) and (50)). These results show that the steady-state signaling rate of the system can easily be made satisfactory regardless of the starting sequence, the initial system conditions, and the time delays in the communication channels. Therefore, there is no need to attempt to activate the two stations simultaneously or to equalize the delays and gains of the communication channels.

In conclusion, the detailed transient and steady-state analyses show that a synchronization system employing digital rate-locked loops can be designed to operate successfully both in the master-to-slave mode and in the slave-to-slave mode. Such a synchronization system, therefore, is useful in applications where both digital and analog transmission facilities are utilized in connecting data stations or other types of terminals.

VI. ACKNOWLEDGMENTS

The author gratefully acknowledges many helpful discussions with J. Salz, J. E. Mazo, R. R. Anderson, D. Hirsch, R. D. Fracassi, F. W. Lescinsky, and C. E. Young.

APPENDIX

In this appendix, we first introduce the concept of equilibrium. The system is said to be in equilibrium if, corresponding to every digit received from Station 2 (the station with master clock), Station 1 (the station with slave clock) also transmits a digit back to Station 2. Then we prove a general theorem which states that the system will reach equilibrium if the arbitrary filter $F(s)$ (not necessarily an RC filter) satisfies a simple condition. Based on this general theorem, we then show that when an RC filter is used, the signaling interval of Station 1 will lock to that of Station 2 exactly.

For brevity, we define $\rho_1(t)$ as $\omega_1 t + \alpha_1 \int_0^t v_1(\tau)d\tau + \theta_1$. The lowpass filter transfer function $F(s)$ can always be normalized such that $F(0) = 1$. Clearly, any useful lowpass filter must cut off as frequency approaches infinity; therefore, we can write $F(\infty) = 0$. By changing units, we can and shall set $e_1 = \pi$ and $\alpha_1 = 1$. Without loss of generality, we assume that $\omega_2 - \omega_1 > 0$, and that the counter counts both upward and downward zero crossings. The zero crossings of $s_1(t)$ and $s_2(t)$ control the signaling rate of Station 1 and Station 2, respectively. Let T be the time interval between each two consecutive zero crossings of $s_2(t)$, that is, $T = \pi/\omega_2$. When the time interval between each two consecutive zero crossings of $s_1(t)$ also becomes T, signaling rate of Station 1 locks to that of Station 2. Thus, to determine the locking behavior, we need only to examine $N_1(t)$ when $t \to \infty$. Since $N_1(t)$ can be deduced from $\rho_1(t)$, $v_1(t)$, or $u_1(t)$, we shall examine either $\rho_1(t)$, or $v_1(t)$, or $u_1(t)$ in the following analysis (depending on which one is the most convenient).

The behavior of the system is governed by the equation

$$\rho_1(t) = \omega_1 t + \int_0^t [f * u_1(\rho_1)]\, d\tau + \theta_1 \tag{55}$$

where * denotes convolution, and the symbol $u_1(\rho_1)$ indicates that u_1 is a function of ρ_1. Since u_1 depends on ρ_1 through the nonlinear zero-crossing counting process, (55) is a nonlinear differential-integral equation. It is impossible to solve this equation for all t, so we shall first examine $v_1(t)$ and $u_1(t)$ to obtain a steady-state solution of this

equation. Then we shall consider the uniqueness of this steady-state solution.

From the mathematical formulation in text,

$$u_1(t) = \left[(\omega_2 - \omega_1)t - \int_0^t v_1(\tau)\, d\tau + \theta_2 - \theta_1 + \psi_1(t) - \psi_2(t)\right]. \quad (56)$$

Let $U_1(s)$, $V_1(s)$, $\Psi_1(s)$, and $\Psi_2(s)$ be the Laplace transforms of $u_1(t)$, $v_1(t)$, $\psi_1(t)$, and $\psi_2(t)$, respectively. From (56) and $V_1(s) = F(s)U_1(s)$, we obtain

$$U_1(s) = \frac{\omega_2 - \omega_1}{s[s + F(s)]} + \frac{\theta_2 - \theta_1}{s + F(s)} + \frac{s}{s + F(s)}\Psi_1(s) - \frac{s}{s + F(s)}\Psi_2(s) \quad (57)$$

and

$$V_1(s) = \frac{F(s)(\omega_2 - \omega_1)}{[s + F(s)]s} + \frac{F(s)(\theta_2 - \theta_1)}{s + F(s)} + \frac{F(s)s}{s + F(s)}\Psi_1(s) - \frac{F(s)s}{s + F(s)}\Psi_2(s). \quad (58)$$

We wish to determine the $N_1(t)$ that satisfies the system equation (55) when $t \to \infty$. For brevity, such a solution is called a steady-state solution. From (58), a steady-state solution is obtained, and is stated in the following theorem.

Theorem 1: At steady-state (that is, when $t \to \infty$), (55) is satisfied if

$$N_1(t) = N_2(t - \tau_0) \quad (59)$$

where τ_0 is such that the mean value of $u_1(t)$ is $\omega_2 - \omega_1$.

Proof: Since $\psi_1(t)$ and $\psi_2(t)$ do not approach a limit when $t \to \infty$, one cannot apply final value theorem to the last two terms in (58). However, final value theorem can be applied to the first two terms. This yields

$$v_1(t) = \omega_2 - \omega_1 + \mathfrak{L}^{-1}\left[\frac{F(s)s}{s + F(s)}\Psi_1(s)\right] - \mathfrak{L}^{-1}\left[\frac{F(s)s}{s + F(s)}\Psi_2(s)\right], \quad t \to \infty. \quad (60)$$

The condition $t \to \infty$ applies to the rest of the proof. Clearly, (59) is equivalent to the statement that

$$\rho_1(t) = \omega_2 t + \tilde{\rho}_1(t) \quad (61)$$

where $\tilde{\rho}_1(t)$ is a periodic function of period T. Thus, to prove Theorem 1, one needs only to show that the right side of (55), when computed

from (59), is identical with the right side of (61). From (59), $\psi_1(t)$ is a periodic function of period T. Consequently, $\mathfrak{L}^{-1}\{[F(s)s/s + F(s)]\Psi_1(s)\}$ is a zero-mean periodic function of period T. Since $\psi_2(t)$ is a period function with period T, $\mathfrak{L}^{-1}\{[F(s)s/s + F(s)]\Psi_2(s)\}$ is also a zero-mean periodic function of period T. Thus, from (60)

$$v_1(t) = \omega_2 - \omega_1 + \bar{v}_1(t) \tag{62}$$

where $\bar{v}_1(t)$ is a zero-mean periodic function with period T. Substituting the $v_1(t)$ in (62) for the integrand $[f * u_1(\rho_1)]$ in (55), we see that the right side of (55) is identical with the right side of (61). This proves Theorem 1.

Equation (59) in Theorem 1 implies that signaling rate of Station 1 locks to that of Station 2. Now we consider the problem of uniqueness (that is, whether (59) is the only steady-state solution). We first prove that, under a simple condition, Station 1 cannot add or delete bits from a customer's data stream.

As described in Section II, the zero crossings of $s_1(t)$ and $s_2(t)$ control the signaling rates of Station 1 and Station 2, respectively. More specifically, Station 2 transmits the mth digit to Station 1 at the mn_0th zero crossing of $s_2(t)$; and Station 1 transmits the mth digit to Station 2 at the mn_0th zero crossing of $s_1(t)$ (in practice, $n_0 \geqq 1$). Thus, Station 2 transmits a digit to Station 1 every n_0T seconds. We say that the system is in equilibrium if, corresponding to every digit received from Station 2, Station 1 also transmits a digit back to Station 2. More precisely, the system is in equilibrium if we can partition the time axis into N_0T-second time intervals such that Station 1 will transmit a digit back to Station 2 in each of the n_0T-second time intervals.

Theorem 2: The system will reach equilibrium if

$$-\pi < \mathfrak{L}^{-1}\left[\frac{s}{s + F(s)}\Psi_1(s)\right] < \pi. \tag{63}$$

Proof: The condition $t \to \infty$ is implied throughout this proof. Using the final-value theorem, one can show from (57) that when $t \to \infty$,

$$u_1(t) = \omega_2 - \omega_1 - \sigma_2(t) + \sigma_1(t) \tag{64}$$

where

$$\sigma_2(t) = \mathfrak{L}^{-1}\left[\frac{s}{s + F(s)}\Psi_2(s)\right] \tag{65}$$

$$\sigma_1(t) = \mathfrak{L}^{-1}\left[\frac{s}{s + F(s)}\Psi_1(s)\right] \tag{66}$$

and $\mathfrak{L}^{-1}$ denotes inverse Laplace transform.

Since $\psi_2(t)$ is periodic with period T, $\sigma_2(t)$ is a zero-mean periodic function of period T. Let max $\sigma_2(t)$ and min $\sigma_2(t)$ be the maximum and minimum value of $\sigma_2(t)$, respectively. We now determine max $\sigma_2(t)$ − min $\sigma_2(t)$. Note that $\psi_2(t)$ can be written as

$$\psi_2(t) = (\omega_2 t + \theta_2) - \sum_i \pi u[t - (t' + iT)] \tag{67}$$

where $u(t)$ is the unit step function defined by

$$\begin{aligned} u(t) &= 0, \quad t < 0 \\ &= 1, \quad t > 0. \end{aligned} \tag{68}$$

When $\psi_2(t)$ is applied to a network with transfer function $[s/s + F(s)]$ (hereafter called network A), the output is $\sigma_2(t)$. Clearly, when the first term $\omega_2 t + \theta_2$ in (67) is applied to network A, the output is a continuous time function for $t > 0$. The second term in (67) consists of unit step functions. It can be shown that, when a unit step function $u(t)$ is applied to network A, the output is unity when $t = 0^+$, approaches zero when $t \to \infty$, and is continuous for $0 < t < \infty$. From these results, it is clear that

$$\max \sigma_2(t) - \min \sigma_2(t) \geqq \pi. \tag{69}$$

We have set $e_1 = \pi$. Therefore, $u_1(t)$ is a multiple of π. We are considering the case $\omega_2 - \omega_1 > 0$. As illustrated in Fig. 7, let n be an integer such that

$$n\pi \leqq \omega_2 - \omega_1 < n\pi + \pi. \tag{70}$$

It is clear from (70) and (69) that there is a t at which $\omega_2 - \omega_1 - \sigma_2(t)$ equals $n\pi$ or $(n + 1)\pi$ (let this t be denoted by t_1). Note that $\omega_2 - \omega_1 - \sigma_2(t)$ may intersect only the level $n\pi$, or only the level $(n + 1)\pi$, or both the levels. For this proof, we need to consider only the first case. Since $\sigma_2(t)$ is periodic with period T, $\omega_2 - \omega_1 - \sigma_2(t)$ is also periodic

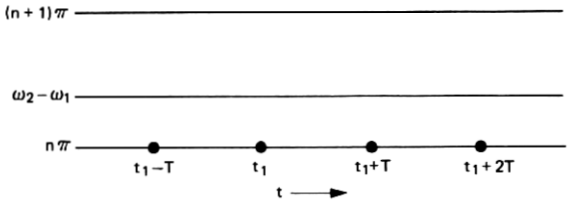

Fig. 7—Illustration for the proof of Theorem 2 (showing the definition of n and the partition of the time axis into successive T-second intervals).

with period T. Thus, $\omega_2 - \omega_1 - \sigma_2(t)$ must intersect the level $n\pi$ also at time instants $t_1 + iT$, $i = \pm 1, \pm 2, \cdots$. These intersections are illustrated in Fig. 7.

Now consider the value of $u_1(t)$ at an intersection $t_1 + iT$, $i = 0, \pm 1, \pm 2, \cdots$. From (63), we have, at $t = t_1 + iT$

$$n\pi - \pi < u_1(t) < n\pi + \pi. \tag{71}$$

Since $u_1(t)$ must be a multiple of π, (71) implies that

$$u_1(t) = n\pi \tag{72}$$

at $t = t_1 + iT$, $i = 0, \pm 1, \pm 2, \cdots$. Since $N_2(t)$ increases by one every T seconds, (72) requires that $N_1(t)$ increase by one in each of the T-second intervals illustrated in Fig. 7. This proves Theorem 2.

Now we consider the case where the filter $F(s)$ is the usual RC filter. We first prove that eq. (63) is satisfied in this case (consequently, the system will reach equilibrium).

When RC filter is used,

$$F(s) = \frac{1}{1 + sCR} \tag{73}$$

$$\frac{s}{s + F(s)} \Psi_1(s) = \Psi_1(s) - \frac{1}{CR(s + r_1)(s + r_2)} \Psi_1(s) \tag{74}$$

where

$$r_1 = \frac{1 + \sqrt{1 - 4CR}}{2CR} \tag{75}$$

$$r_2 = \frac{1 - \sqrt{1 - 4CR}}{2CR}. \tag{76}$$

The system is designed such that

$$1 - 4CR > 0. \tag{77}$$

Therefore r_1 and r_2 are real numbers and

$$r_1 > r_2 > 0. \tag{78}$$

Let $[1/CR(s + r_1)(s + r_2)]$ be denoted by $G(s)$, then

$$g(t) = \mathcal{L}^{-1}[G(s)] = \frac{1}{CR(r_1 - r_2)} [e^{-r_2 t} - e^{-r_1 t}]. \tag{79}$$

From (78) and (79),

$$g(t) > 0, \quad t > 0. \tag{80}$$

From (80), we can write

$$\mathcal{L}^{-1}[\Psi_1(s)G(s)] = \int_0^t \psi_1(\tau)g(t-\tau)\,d\tau < \int_0^t \pi g(t-\tau)\,d\tau < \int_0^\infty \pi g(\tau)\,d\tau. \tag{81}$$

Clearly, $\int_0^\infty g(\tau)d\tau = G(0) = 1$. From this and (81), we have

$$0 < \mathcal{L}^{-1}[\Psi_1(s)G(s)] < \pi. \tag{82}$$

From (82) and (74)

$$-\pi < \mathcal{L}^{-1}\left[\frac{s}{s+F(s)}\Psi_1(s)\right] < \pi. \tag{83}$$

Hence, (63) is satisfied and the system will reach equilibrium.

Next, we examine the detailed behavior of the rate-locked loop. Note that there are two basic variables in the rate-locked loop, namely, $u_1(t)$ and $v_1(t)$. Let the $u_1(t)$ and $v_1(t)$ corresponding to the steady-state solution in (59) be denoted by $u_1^*(t)$ and $v_1^*(t)$, respectively. First, we sketch $u_1^*(t)$ and $v_1^*(t)$. From Section II in text, $s_2(t) = \sin[\omega_2 t + \theta_2]$. To simplify our graphs, let us omit θ_2. Then $N_2(t)$ jumps by 1 at $t = lT$, $l = 0, 1, 2, \cdots$. From this and (59), we see that $u_1^*(t)$ is as sketched in Fig. 8, where l denotes an arbitrary integer. The pulse width y^* in Fig. 8 is such that the mean-value of $u_1^*(t)$ is $\omega_2 - \omega_1$. Therefore,

$$y^* = \frac{T}{\pi}[\omega_2 - \omega_1 - n\pi]. \tag{84}$$

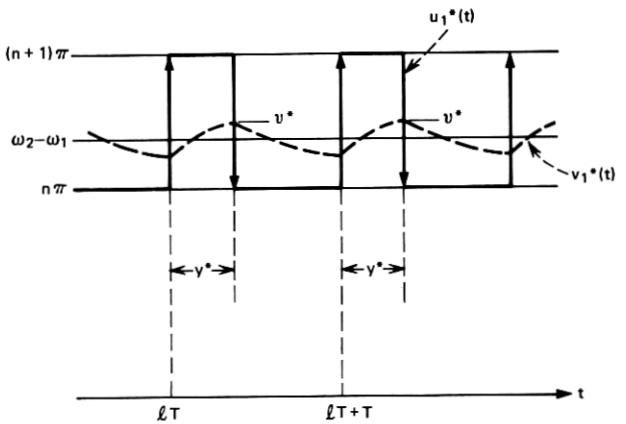

Fig. 8—Sketch of $u_1^*(t)$ and $v_1^*(t)$.

Since $u_1^*(t)$ is periodic with period T, $v_1^*(t)$ is also periodic with period T. As can be seen from $v_1^*(t)$ in Fig. 8, $u_1^*(t)$ charges the capacitor C in the time interval lT to $lT + y^*$, and the capacitor C discharges in the time interval $lT + y^*$ to $lT + T$. Let ν^* denote the value of $v_1^*(t)$ at $t = lT + y^*$. Clearly, ν^* must have such a value that $v_1^*(t)$ has a mean-value of $\omega_2 - \omega_1$.

In order to show that $u_1^*(t)$ and $v_1^*(t)$ are the only steady-state solution, we begin by assuming different $u_1(t)$ and $v_1(t)$, and demonstrate that they must approach $u_1^*(t)$ and $v_1^*(t)$ as t increases. We have proved that the system must reach equilibrium. From (72), when the system reaches equilibrium, $u_1(t) = n\pi$ at $t = t_1 + iT$, $i = 0, \pm 1, \pm 2, \cdots$. [As can be seen from the discussion after (70), $u_1(t)$ may assume the other value $(n + 1)\pi$ at such time instants. However, these two cases are similar and we need to consider only the first case.] Therefore, $u_1(t)$ can assume only one of the two forms in Fig. 9 in each of the time intervals $t_1 + iT$ to $t_1 + iT + T$. The first form is illustrated in the time interval t_1 to $t_1 + T$ in Fig. 9, while the second form is illustrated in the time interval $t_1 + T$ to $t_1 + 2T$. In the first form, the zero crossing of $s_1(t)$ (represented by the downward arrow) takes place prior to the zero crossing of $s_2(t)$ (represented by the upward arrow). The order is reversed in the second form. Note that, if $u_1(t)$ always assumes the first form, one would have $v_1(t) < n\pi$. From this, one can easily show that $u_1(t)$ cannot always assume the first form in the successive T-second intervals. Next, consider the width of the pulse when $u_1(t)$

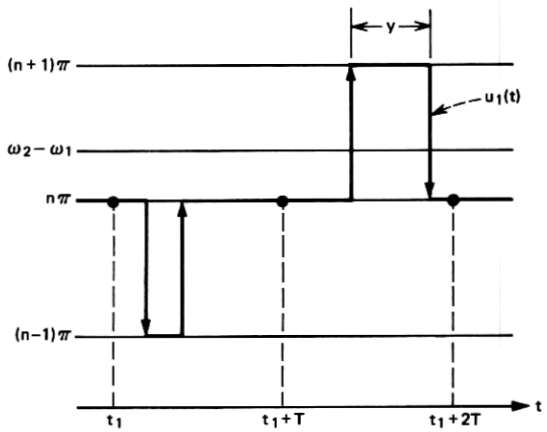

Fig. 9—Illustration of the two forms of $U_1(t)$.

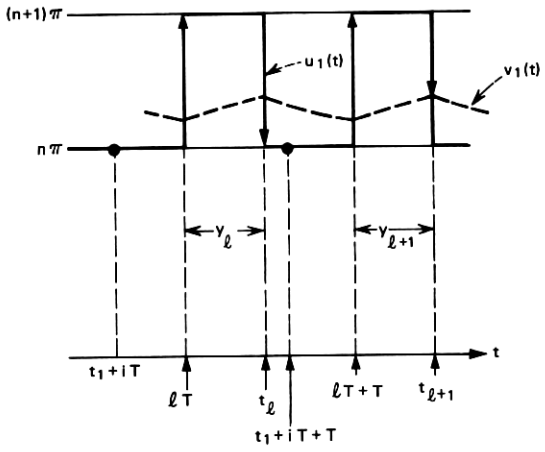

Fig. 10—Sketch of $u_1(t)$ and $v_1(t)$.

assumes the second form. This width, designated by y in Fig. 9, may vary from one T-second interval to the next. If this width were always less than y^*, $v_1(t)$ would be less than v^* for all t. From this, one can show that this width cannot always be less than y^*. From these results, there must be some T-second intervals in which $u_1(t)$ assumes the second form and the pulse width y is equal to or greater than y^*. We shall select one such time interval (say, the time interval $t_1 + iT \leqq t < t_i + iT + T$ illustrated in Fig. 10) and examine $u_1(t)$ and $v_1(t)$ for $t > t_1 + iT$. We need to consider only two cases (refer to Fig. 10):

$$\text{Case 1:} \quad v_1(t_l) < v^*$$

$$\text{Case 2:} \quad v_1(t_l) \leqq v^*.$$

The instantaneous radian frequency of VCO_1 is $\omega_1 + \alpha_1 v_1(t)$, where ω_1 is the free-running radian frequency and $\alpha_1 v_1(t)$ is the correction term. In data communications, ω_1 is very close to the radian frequency ω_2 of the master clock. (For example, it may be specified that the maximum difference between ω_1 and ω_2 be limited to 0.005 percent of ω_2.) Consequently, only a very small correction term $\alpha_1 v_1(t)$ is needed. For this season, the time interval between each two consecutive zero crossings of $s_1(t)$ is essentially determined by the term $\omega_1 t$ in $\rho_1(t)$. Therefore, the pulse width y changes only very slightly from one pulse to the next (in other words, in Fig. 10 y_{l+1} is very close to y_l).

For the purpose of illustration, in Fig. 10 $v_1(t)$ is shown to increase

and decrease quite rapidly in each T-second interval. In practice, the filter time constant RC is several orders larger than the time interval T (for example, $RC = 10^{-1}$ seconds, $T \cong 10^{-5}$ seconds). Thus, $v_1(t)$ is essentially a constant in each T-second time interval.

Now consider y_{l+j} and $v_1(t_{l+j})$, $j = 1, 2, 3, \cdots$. It can be shown rigorously that if there is an h such that

$$y_{l+h} = y^*$$
$$v_1(t_{l+h}) = \nu^*$$

then $y_{l+j} = y^*$ and $v_1(t_{l+j}) = \nu^*$ for all $j > h$. Therefore, to show that $u_1(t)$ and $v_1(t)$ approach $u_1^*(t)$ and $v_1^*(t)$, we need only show that y_{l+j} and $v_1(t_{l+j})$ approach y^* and ν^*, respectively.

Now consider Case 1; after $t_1 + iT$, y_{l+j} and $v_1(t_{l+j})$ approach y^* and ν^* in three stages. Immediately after $t_1 + iT$, $v_1(t_{l+j})$ is less than ν^*. Consequently, the time interval between each two consecutive zero crossings of $s_1(t)$ is slightly larger than T, and y_{l+j} increases slowly with j. (Note from Theorem 2 that y_{l+j} must remain less than T.) Since $v_1(t_{l+j})$ is less than ν^* and y_{l+j} remains larger than y^*, $v_1(t_{l+j})$ must increase slowly with j. The second stage starts when $v_1(t_{l+j})$ reaches ν^*. Since the pulse width y_{l+j} is larger than y^*, $v_1(t_{l+j})$ keeps increasing with j. (Note from Theorem 2 that $v_1(t_{l+j})$ cannot exceed $(n + 1)\pi$.) This implies that $v_1(t_{l+j})$ will be larger than ν^*. Consequently, y_{l+j} must decrease with j. Clearly, when y_{l+j} decreases, the rate of increase of $v_1(t_{l+j})$ decreases. The third stage starts when y_{l+j} decreases to such a value (still larger than y^*) that $v_1(t_{l+j})$ ceases increasing. Since $v_1(t_{l+j})$ is now larger than ν^*, y_{l+j} must keep decreasing. Clearly, this must also reduce $v_1(t_{l+j})$. Consequently, y_{l+j} and $v_1(t_{l+j})$ approach y^* and ν^*, respectively.

The above discussion is for Case 1. It can easily be extended to Case 2. Thus, when the system reaches equilibrium, the time interval between each two consecutive zero crossings of $s_1(t)$ will be exactly T seconds.

REFERENCES

1. Gardner, F. M., *Phaselock Techniques*, New York: John Wiley and Sons, Inc., 1966, p. 65.
2. Gersho, A., and Karafin, B. J., "Mutual Synchronization of Geographically Separated Oscillators," B.S.T.J., *45*, No. 10 (December 1966), pp. 1689–1704.
3. Karnaugh, M., "A Model for the Organic Synchronization of Communication Systems," B.S.T.J., *45*, No. 10 (December 1966), pp. 1705–1736.
4. Brilliant, M. B., "The Determination of Frequency in Systems of Mutually Synchronized Oscillators," B.S.T.J., Vol. *45*, No. 10 (December 1966), pp. 1737–1748.

5. Williard, M. W., "Analysis of a System of Mutually Synchronized Oscillators," IEEE Trans. Commun. Tech., *COM-18*, No. 5 (October 1970), pp. 467–483.
6. Williard, M. W., and Dean, H. R., "Dynamic Behavior of a System of Mutually Synchronized Oscillators," IEEE Trans. Commun. Tech., *COM-19*, No. 4 (August 1971), pp. 373–395.
7. Saito, T., "Dynamic Characteristics of Mutually Synchronized Systems," Elec. Commun. Japan, *51-A*, No. 4, 1968, pp. 19–27.
8. West, N., "Synchronous Digital Switching in Highly Interconnected Communication Networks," Proc. Inst. Elec. Eng., *114*, No. 10 (October 1967*e*, pp. 1378–1384.
9. Chang, R. W., Mazo, J. E., and Salz, J., "Stability Analysis of a Digital Rate-Lock Loop," unpublished work.
10. Chang, R. W., unpublished work.